

# The Seventh Most Referenced Transactions Paper of the EMC Society

*Daniel D. Hoolihan, History Committee Chair*

## INTRODUCTION

As the devoted readers of the History section of the EMC Newsletter know, as a carryover to the 50th Anniversary Celebration of the EMC Society of the IEEE (1957-2007), we are republishing past top papers in the *IEEE Transactions on Electromagnetic Compatibility*. In the six previous Newsletters, we have published the first six most referenced papers, which are, respectively:

1. "Transient Response of Multiconductor Transmission Lines Excited by a Nonuniform Electromagnetic Field;" EMC-22, No. 2, May – 1980, Page 119 by A. K. Agrawal, H. J. Price, and S. H. Gurbaxani.
2. "Absorbing Boundary Conditions for the Finite-Difference Approximation of the Time-Domain Electromagnetic Field Equations;" EMC-23, No. 4, November – 1981, Page 377 by Gerrit Mur.
3. "Generation of Standard Electromagnetic Fields Using TEM Transmission Cells;" EMC-16, No. 4, November – 1974, Pages 189 -195 by Myron (Mike) L. Crawford.
4. "Frequency Response of Multiconductor Transmission

Lines Illuminated by an Electromagnetic Field," EMC-18, No. 4, November – 1976, Pages 183-190 by Clayton R. Paul.

5. "Statistical Model for a Mode-Stirred Chamber," EMC-33, No. 4, November – 1991, Pages 366-370 by Joseph G. Kostas and Bill Boverie.
6. "Correction of Maxwell's Equations for Signals I," EMC-28, No. 4, November -1986, Pages 250-258 by Henning Harmuth.

In this issue, we are publishing the seventh Most-Referenced EMC Society Transactions paper of the first fifty years of the EMC Society and it is written by Dennis A. Hill, Mark T. Ma, Arthur R. Ondrejka, Bill F. Riddle, Myron L. Crawford, and Robert T. Johnk.

The title of the paper is "Aperture Excitation of Electrically Large, Lossy Cavities" and it was first published in the *IEEE Transactions on EMC* in Volume 36, No. 3 in August 1994.

Again, we hope you take the time to read and appreciate the significance of this historical technical article.

# Aperture Excitation of Electrically Large, Lossy Cavities

David A. Hill, *Fellow, IEEE*, Mark T. Ma, *Fellow, IEEE*, Arthur R. Ondrejka, Bill F. Riddle, Myron L. Crawford, *Fellow, IEEE*, and Robert T. Johnk, *Member, IEEE*

**Abstract**—We present a theory based on power balance for aperture excitation of electrically large, lossy cavities. The theory yields expressions for shielding effectiveness, cavity  $Q$ , and cavity time constant. In shielding effectiveness calculations, the incident field can be either a single plane wave or a uniformly random field to model reverberation chamber or random field illumination. The  $Q$  theory includes wall loss, absorption by lossy objects within the cavity, aperture leakage, and power received by antennas within the cavity. Extensive measurements of shielding effectiveness, cavity  $Q$ , and cavity time constant were made on a rectangular cavity, and good agreement with theory was obtained for frequencies from 1 to 18 GHz.

## I. INTRODUCTION

IN MANY electromagnetic interference (EMI) problems, the important electronic systems are located within a metal enclosure with apertures. In such cases it is important to know the shielding effectiveness (SE) of the enclosure so that we can relate the interior fields to the external incident fields. For example, the high-intensity radiated fields (HIRF's) suggested in SAE draft advisory circular AE4R [1] are in the 1000- to 7000-V/m range for frequencies above 400 MHz, the frequencies used by most radars. However, the shielding effectiveness of aircraft skins is not well known, so the interior fields that excite the aircraft electronics are not well characterized.

The purpose of this paper is to develop a mathematical model for the shielding effectiveness of electrically large enclosures that contain apertures and interior loading. The method that we present uses a power balance approach and yields a simple, approximate expression for the average field strength throughout the cavity enclosed by the enclosure. This method does not yield the fine detail of the interior fields as would be obtained by a numerical method [2], but it has the advantages of being applicable to both CW and pulsed RF fields and not requiring all the geometrical details of the enclosure, the apertures, and the loads. The theory is similar to that developed for reverberation chambers [3]–[5], where the average power density is assumed to be uniform throughout the chamber.

The organization of this paper is as follows. Section II contains a derivation for the cavity quality factor ( $Q$ ) of an electrically large cavity where the losses include skin effect in

Manuscript received October 14, 1993; revised February 24, 1994. This research was supported by the Federal Aviation Administration.

The authors are with the Electromagnetic Fields Division, National Institute of Standards and Technology, Boulder, Colorado 80303 USA.  
IEEE Log Number 9401880.

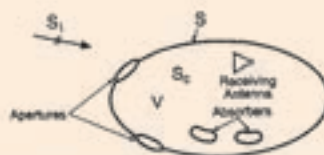


Fig. 1. Aperture excitation of a cavity containing absorbers and a receiving antenna.

the walls, volume absorption by lossy objects within the cavity, leakage through apertures, and power absorbed by receiving antennas. Section III covers aperture excitation of the cavity by an external field. Section IV contains a power balance derivation of the shielding effectiveness and the time constant of the cavity. Section V presents measurement methods and comparisons of measured and theoretical values of SE,  $Q$ , and the time constant. Section VI presents conclusions and recommendations for further work. A longer report [6] that includes further details of the mathematics and measurements is available from the authors.

## II. CAVITY QUALITY FACTOR

The  $Q$  of a cavity is a key quantity in calculating both SE of the surrounding shield and the time constant of the cavity. We consider an electrically large (multimode) cavity as shown in Fig. 1. In general, the cavity will have apertures and will contain lossy objects and at least one receiving antenna. The definition for  $Q$  is

$$Q = \omega U_s / P_d \quad (1)$$

where  $\omega$  is the excitation (angular) frequency,  $U_s$  is the steady-state energy in the cavity, and  $P_d$  is the dissipated power. In our application, the cavity is excited by an exterior field incident on apertures, but the  $Q$  theory does not depend on the excitation method. Thus this theory is also applicable to reverberation chambers excited by antennas.

We can write the steady-state energy  $U_s$  as the product of the energy density  $W$  times the cavity volume  $V$

$$U_s = WV. \quad (2)$$

In (2) we assume that  $W$  is uniform throughout the cavity volume, and this uniformity has been shown for the average energy density in reverberation chambers [4]. In reverberation

chamber measurements, an ensemble average is obtained by rotating a mode stirrer, and in our theory we deal with ensemble averages that could represent averages over different cavity shapes. It is useful to write  $W$  in terms of the rms electric field  $E$

$$W = \epsilon_0 E^2 \quad (3)$$

where  $\epsilon_0$  is the permittivity of free space and we have assumed the stored electric and magnetic energies are equal.  $E^2$  should also be interpreted as an ensemble average. It is also useful to write an expression for the power density  $S_c$  within the cavity

$$S_c = E^2/\eta_0 = cW \quad (4)$$

where  $\eta_0 = (\mu_0/\epsilon_0)^{1/2}$ ,  $c = 1/(\mu_0\epsilon_0)^{1/2}$ , and  $\mu_0$  is the magnetic permeability of free space.  $S_c$  should also be interpreted as an ensemble average.

The dissipated power can be written as the sum of four terms

$$P_d = P_{d1} + P_{d2} + P_{d3} + P_{d4} \quad (5)$$

where  $P_{d1}$  is the power dissipated in the cavity walls,  $P_{d2}$  is the power absorbed in loading objects within the cavity,  $P_{d3}$  is the power lost through aperture leakage, and  $P_{d4}$  is the power dissipated in the loads of receiving antennas. The forms of (1) and (5) suggest that we write an expression for the inverse of  $Q$

$$Q^{-1} = Q_1^{-1} + Q_2^{-1} + Q_3^{-1} + Q_4^{-1}, \quad (6)$$

where

$$Q_1 = \omega U_s/P_{d1}, \quad Q_2 = \omega U_s/P_{d2}, \quad Q_3 = \omega U_s/P_{d3}$$

and

$$Q_4 = \omega U_s/P_{d4}. \quad (7)$$

The smallest of  $Q_1, Q_2, Q_3$ , and  $Q_4$  will be the dominant contributor to  $Q$ . We now consider the individual loss mechanisms.

#### A. Wall Losses

For highly conducting walls the wall loss can be determined from the skin depth approximation. For reverberation chambers, the wall loss has been determined both by averaging over the individual cavity modes [7] and by averaging plane-wave losses over all incidence angles and polarizations [5]. The latter approach is consistent with our ensemble average theory. In either case, the result for  $Q$  is

$$Q_1 = \frac{3V}{2\mu_r S\delta} \quad (8)$$

where

$$\delta = (2/\omega\mu_w\sigma_w)^{1/2}, \quad \mu_r = \mu_w/\mu_0$$

and where  $S$  is the cavity surface area,  $\delta$  is the skin depth,  $\mu_w$  is the wall permeability, and  $\sigma_w$  is the wall conductivity.

Complications, such as variations in wall conductivity and permeability with position, could also be treated using the skin depth approximation, but the skin depth would then be a function of position. Wall coatings, such as paint, could also be included, but we would still lump all wall losses into  $Q_1$ .

#### B. Absorption

In general, the absorption cross section  $\sigma_a$  of a lossy object depends on the incidence angle and polarization of the incident plane wave [8]. Since we assume that the fields in an electrically large cavity can be written as a superposition of plane waves of all incidence angles and polarizations [9], the absorbed power can be written as the product of the cavity power density  $S_c$  and the averaged absorption cross section  $\langle\sigma_a\rangle$

$$P_{d2} = S_c\langle\sigma_a\rangle \quad (9)$$

where  $\langle\ \rangle$  indicates an incidence angle average over  $4\pi$ , steradians and an average over all polarizations.

The absorption cross section in (9) can be that of a single object or a summation for a number of absorbers. For example, for  $M$  absorbers  $\langle\sigma_a\rangle$  in (9) would be replaced by

$$\langle\sigma_a\rangle = \sum_{i=1}^M \langle\sigma_{ai}\rangle \quad (10)$$

where  $\langle\sigma_{ai}\rangle$  is the averaged absorption cross section of the  $i$ th absorber. For the example of an aircraft, the  $i$  summation in (10) could represent absorption by people, seats, wiring, etc.

For the simple case of a uniform sphere, the absorption cross section is independent of the incidence angle and polarization of the incident field and no averaging is required. The cross-section formulation for a uniform sphere is given in [6] and [8].

If we use (2), (4), (7), and (9), we can derive the following expression for  $Q_2$ :

$$Q_2 = \frac{2\pi V}{\lambda\langle\sigma_a\rangle} \quad (11)$$

where  $\lambda$  is the free-space wavelength. The frequency dependence of  $Q_2$  can be fairly complicated because of the frequency dependence of  $\langle\sigma_a\rangle$ . (See [8] for the frequency dependence of the absorption cross section of a homogeneous sphere.)

#### C. Aperture Leakage

In general, the transmission cross section  $\sigma_t$  of an aperture depends on the incidence angle and polarization of the incident plane wave [10]. We again assume that the fields can be written as a superposition of plane waves of all incidence angles and polarizations, but only the plane waves that propagate toward the apertures contribute to the transmitted power. Consequently, we introduce a factor of 1/2 in the product expression for the leakage power

$$P_{d3} = S_c\langle\sigma_t\rangle/2 \quad (12)$$

where  $\langle \rangle$  represents an incidence angle average over  $2\pi$ , steradians (including only plane waves from the cavity side) and an average over polarization.

The transmission cross section in (12) can be that of a single aperture or a summation for a number of apertures. For  $N$  apertures,  $\langle \sigma_t \rangle$  in (12) would be replaced by

$$\langle \sigma_t \rangle = \sum_{i=1}^N \langle \sigma_{ti} \rangle \quad (13)$$

where  $\langle \sigma_{ti} \rangle$  is the averaged transmission cross section of the  $i$ th aperture. For the example of an aircraft, the  $N$  summation in (13) could represent leakage through windows and other apertures of different shapes and sizes. Specific expressions for transmission cross sections are given in Section III.

If we use (2), (4), (7), and (13), we can derive the following expression for  $Q_3$ :

$$Q_3 = \frac{4\pi V}{\lambda \langle \sigma_t \rangle} \quad (14)$$

For electrically large apertures,  $\langle \sigma_t \rangle$  is independent of frequency, and  $Q_3$  is proportional to frequency. For small or resonant apertures, the frequency dependence of  $Q_3$  is more complicated.

#### D. Receiving Antenna

The power  $P_{d4}$  dissipated in the load of the receiving antenna can be written as the product of the cavity power density and the averaged effective area of the receiving antenna

$$P_{d4} = S_c \langle A_e \rangle \quad (15)$$

where the effective area  $A_e$  is also averaged over incidence angle and polarization. The average effective area  $\langle A_e \rangle$  of a lossless antenna can be written as the product of the effective area of an isotropic antenna ( $\lambda^2/4\pi$ ), the impedance mismatch factor  $m$ , and a polarization mismatch factor of 1/2 [11], [12]

$$\langle A_e \rangle = \frac{m\lambda^2}{8\pi} \quad (16)$$

$\langle A_e \rangle$  in (16) does not depend on the antenna pattern because it is averaged over all possible incidence angles and polarizations [9]. The impedance mismatch factor  $m$  is equal to 1 for a matched load and is less than 1 otherwise.

If we use (2), (4), (7), (15), and (16), we can derive the following expression for  $Q_4$ :

$$Q_4 = \frac{16\pi^2 V}{m\lambda^3} \quad (17)$$

If there is more than one receiving antenna in the cavity, then  $\langle A_e \rangle$  in (15) is replaced by a sum of averaged effective areas. For a matched load ( $m = 1$ ),  $Q_4$  is proportional to frequency cubed. This means that  $Q_4$  is small for low frequencies and is the dominant contributor to the total  $Q$  in (6). The effect of antenna loading on the  $Q$  of reverberation chambers has

been observed experimentally [13]. At high frequencies,  $Q_4$  becomes large and contributes little to the total  $Q$ .

### III. APERTURE EXCITATION

Consider a CW plane wave of power density  $S_i$  incident on the shield apertures as shown in Fig. 1. If the total transmission cross section of the apertures is  $\sigma_t$ , the power  $P_t$  transmitted into the cavity is

$$P_t = \sigma_t S_i \quad (18)$$

(Of course, power will also leak out through the apertures, but we lump that effect under leakage loss  $P_{L3}$  as discussed in Section II-C.) For the general case of  $N$  apertures,  $\sigma_t$  can be written as a sum

$$\sigma_t = \sum_{i=1}^N \sigma_{ti} \quad (19)$$

where  $\sigma_{ti}$  is the transmission cross section of the  $i$ th aperture. In general,  $\sigma_{ti}$  and  $\sigma_t$  depend on the frequency, incidence angle, and polarization of the incident field.

If the shielded cavity is illuminated in a reverberation chamber (random illumination), then the transmitted power can be written

$$P_t = \langle \sigma_t \rangle S_i / 2 \quad (20)$$

The factor 1/2 in (20) results from shadowing of the incident field by the electrically large enclosure and is a good approximation for convex shields. The remaining average  $\langle \rangle$  is over  $2\pi$ , steradians and polarization. The average value of the transmission cross section for  $N$  apertures is obtained directly from (19).

$$\langle \sigma_t \rangle = \sum_{i=1}^N \langle \sigma_{ti} \rangle \quad (21)$$

The results in (20) and (21) could also be used in applications where the incidence angle and polarization are unknown.

#### A. Apertures of Arbitrary Shape

Consider a plane wave incident on an aperture in a perfectly conducting sheet as shown in Fig. 2. For convenience, we drop the subscript  $i$  that identifies the  $i$ th aperture in the shield. Aperture theory has been developed primarily for apertures in flat, perfectly conducting screens of infinite extent and zero thickness [10]. Here we assume that the shield is locally planar and that the shield thickness is small. Aperture theory can be subdivided into three cases where the aperture dimensions are either small, comparable, or large compared to the wavelength.

For electrically large apertures, the geometrical optics approximation yields

$$\sigma_t = A \cos \theta^i \quad (22)$$

where  $A$  is the aperture area and  $\theta^i$  is the incident elevation angle. Thus  $\sigma_t$  is independent of frequency, polarization,

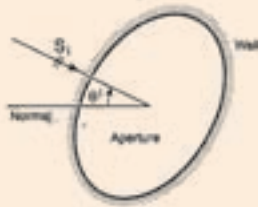
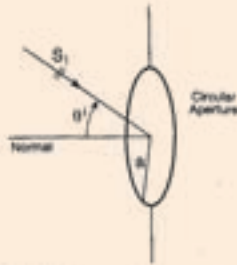


Fig. 2. External field incident on an aperture of arbitrary shape.

Fig. 3. External field incident on a circular aperture of radius  $a$ .

and azimuth of the incident field. For this case, the average transmission cross section can be written

$$\langle \sigma_t \rangle = \frac{1}{2\pi} \int_0^{2\pi} d\phi^i \int_0^{\pi/2} d\theta^i A \cos \theta^i \sin \theta^i = A/2 \quad (23)$$

where we restrict  $\theta^i$  to angles less than  $\pi/2$  because the field is incident from only one side of the screen.

For electrically small apertures, polarizability theory states that the transmitted fields are those of induced electric and magnetic dipole moments [10], [14]. This theory yields a transmission cross section that is proportional to frequency to the fourth power

$$\sigma_t = Ck^4 \quad (24)$$

where  $C$  depends on incident angle and polarization and aperture size and shape, but is independent of frequency. The wavenumber  $k = \omega/c$ . The specific form of  $C$  for a circular aperture will be given in the following section.

In the resonance region, the aperture dimensions are comparable to a wavelength, and the frequency dependence of  $\sigma_t$  depends on the aperture shape. Numerical methods [10] can be used to compute  $\sigma_t$  for such cases, but we will not pursue such methods here.

### B. Circular Aperture

The circular aperture is of particular interest because it has an analytical solution and it is easy to work with experimentally. The geometry for a circular aperture of radius  $a$  is shown in Fig. 3. An exact solution for the transmission coefficient is available in terms of spheroidal functions [15], but we choose to construct a simpler solution in terms of the simple approximations that are available for electrically large and small circular apertures.

For electrically large circular apertures, the geometrical optics approximations in (22) and (23) yield the following

expressions for the transmission cross section and the averaged transmission cross section

$$\sigma_t = \pi a^2 \cos \theta^i \quad \text{and} \quad \langle \sigma_t \rangle = \pi a^2 / 2. \quad (25)$$

For electrically small circular apertures, polarizability theory [10] can be used to determine the effective electric and magnetic dipole moments and the resultant transmission cross section. The details are given in Appendix 1. The transmission cross section depends on the polarization and the elevation angle of the incident field. For the electric field polarized parallel to the incidence plane (defined by the incident wave vector and the normal to the aperture), we write the transmission cross section as  $\sigma_{t \text{ par}}$

$$\sigma_{t \text{ par}} = \frac{64}{27\pi} k^4 a^6 \left(1 + \frac{1}{4} \sin^2 \theta^i\right). \quad (26)$$

For perpendicular polarization, we write the transmission cross section as  $\sigma_{t \text{ perp}}$

$$\sigma_{t \text{ perp}} = \frac{64}{27\pi} k^4 a^6 \cos^2 \theta^i. \quad (27)$$

Both  $\sigma_{t \text{ par}}$  and  $\sigma_{t \text{ perp}}$  have the  $k^4$  dependence given by (24), and they are equal for normal incidence ( $\theta^i = 0$ ). We assume that an incident random field will have equal power densities in the parallel and perpendicular waves. Thus the averaged transmission cross section can be written

$$\langle \sigma_t \rangle = \frac{1}{2} \int_0^{\pi/2} d\theta^i (\sigma_{t \text{ par}} + \sigma_{t \text{ perp}}) \sin \theta^i \quad (28)$$

where we have used the fact that the transmission cross sections are independent of the incident azimuth angle. If we substitute (26) and (27) into (28) and carry out the integration over  $\theta^i$ , we obtain

$$\langle \sigma_t \rangle = \frac{16}{9\pi} k^4 a^6. \quad (29)$$

We do not have a simple expression for the transmission cross section that is valid in the resonance region, but the circular aperture does not have strong resonances [16]. Thus we choose to cover the entire frequency range by using only the electrically small and electrically large approximations. The crossover wavenumber  $k_c$  where we switch from (29) to (25) for the average transmission cross sections is given by equating (25) and (29)

$$\pi a^2 / 2 = \frac{16}{9\pi} k_c^4 a^6. \quad (30)$$

The solution to (30) is

$$k_c a = (9\pi^2 / 32)^{1/4} \approx 1.29. \quad (31)$$

This technique is not valid for long, narrow apertures, which typically have strong resonances.

## IV. POWER BALANCE

## A. Shielding Effectiveness

Consider again the geometry in Fig. 1, where an incident wave is incident on a shielded cavity with apertures. We wish to determine the power density  $S_c$  inside the cavity. For steady-state conditions, we require that the power  $P_i$  transmitted through the apertures is equal to the power  $P_d$  dissipated in the four loss mechanisms considered in Section II

$$P_i = P_d. \quad (32)$$

If we substitute (1), (2), (4), and (18) into (32), we can solve for the power density  $S_c$  in the cavity

$$S_c = \frac{\sigma_t \lambda Q}{2\pi V} S_i. \quad (33)$$

Since we have assumed that the power density  $S_c$  is uniform throughout the cavity, we can define shielding effectiveness in terms of the ratio of the incident and cavity power densities

$$SE = 10 \log_{10} (S_i/S_c) = 10 \log_{10} \left( \frac{2\pi V}{\sigma_t \lambda Q} \right) \text{ dB}. \quad (34)$$

The results in (33) and (34) are consistent with a recent treatment of a related problem [17]. We have defined SE to be a positive number when the cavity power density is less than the incident power density. Our definition of SE in (34) depends on the cavity volume and  $Q$  in addition to the transmission cross section  $\sigma_t$ .

The results in (33) and (34) apply to a single incident plane wave where  $\sigma_t$  depends on the incident direction and polarization. For the case of uniformly random incidence (as in a reverberation chamber), we need to replace  $\sigma_t$  in (33) and (34) by one-half the averaged value  $\langle \sigma_t \rangle / 2$ .

The  $Q$  enhancement of the cavity power density is clear in (33) and (34), and we can see that a lossy cavity (low- $Q$ ) has a greater shielding effectiveness than a high- $Q$  cavity. The importance of loss is seen if we consider the special case where the cavity is lossless ( $P_{d1} = P_{d2} = P_{d3} = 0$ ) except for leakage. In this case  $Q$  is given by

$$Q = Q_3 = \frac{4\pi V}{\lambda \langle \sigma_t \rangle}. \quad (35)$$

If we substitute (35) into (33), we obtain

$$S_c = S_i \frac{2\sigma_t}{\langle \sigma_t \rangle}. \quad (36)$$

For the case of uniformly random excitation, the transmission cross section is replaced by one half the averaged cross section. However, the averaged transmission cross section is equal to the averaged leakage cross section ( $\langle \sigma_t \rangle = \langle \sigma_l \rangle$ ), and (36) reduces to

$$S_c = S_i \text{ or } SE = 0 \text{ dB}. \quad (37)$$

Thus the leakage loss equals the transmitted power, and the cavity has zero shielding. This result is independent of the aperture size and shape. Physically, this case corresponds to an

apertured (but otherwise lossless) cavity inside a reverberation chamber. We expect actual aircraft cavities to have significant loss and fairly low  $Q$ .

## B. Time Constant

Up to this point we have considered only steady-state, single-frequency excitation. Since radar pulses are important in aircraft applications, we also need to consider transient effects. In general, this is a complex problem that is best handled using Fourier integral techniques. However, we can analyze the special case of a turned-on or turned-off sinusoid in a simpler manner.

We consider first the case of field decay where the source (the incident power density) is instantaneously turned off. By equating the change in the cavity energy  $U$  to the negative of the dissipated power times a time increment  $dt$ , we obtain the differential equation

$$dU = -P_d dt. \quad (38)$$

We can use (1) to replace  $P_d$  in (38)

$$dU = -(\omega U/Q) dt = -\frac{U}{\tau} dt \quad (39)$$

where the time constant  $\tau = Q/\omega$ . The initial condition is  $U = U_s$  at  $t = 0$ . The solution of (39) with this initial condition is

$$U = U_s e^{-t/\tau}, \quad t > 0. \quad (40)$$

The closely related case of a turned-on (step-modulated) incident power density involves the same exponential function and time constant

$$U = U_s (1 - e^{-t/\tau}), \quad t > 0. \quad (41)$$

The cavity energy density and power density also follow the same exponential variation with the same time constant, and (40) and (41) agree with [3]. If a radar pulse duration is long compared to  $\tau$ , then the cavity fields will reach their steady-state value. However, if the pulse length is short compared to  $\tau$ , the fields will not reach their steady-state values before the incident pulse is turned off. Some common radars and their pulse characteristics are described in [6].

A high- $Q$  (long- $\tau$ ) cavity might have poor steady-state SE, but would require a long time for the cavity fields to reach their steady-state values. Physically, a high  $Q$  (long  $\tau$ ) means that waves make many bounces within the cavity before they decay.

## C. Source Inside Cavity

We can use the power balance theory of Section IV-A to analyze the case of an internal source, a transmitting antenna located within the cavity. This configuration is of interest in calculating either the power density within an aircraft caused by unintentional emitters or the power density within a reverberation chamber with loading.

If a CW source within the cavity transmits power  $P_i$ , then (32) still holds, but  $P_i$  now represents antenna transmitted power rather than aperture transmitted power. As with aperture

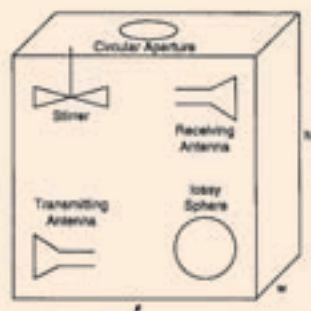


Fig. 4. Rectangular cavity with a circular aperture, a mode stirrer, receiving and transmitting antennas, and lossy sphere(s).

excitation, there is no need to calculate the fields scattered by the cavity walls. Using (1), (2), (4), and (32), we can solve for the power density  $S_c$  within the cavity

$$S_c = \frac{\lambda Q P_t}{2\pi V} \quad (42)$$

Equation (42) applies to cavities with general loading because  $Q$  includes all of the loss mechanisms discussed in Section II, including any power absorbed by the receiving and transmitting antennas.

If an impedance-matched, receiving antenna is placed within the cavity, then the received power  $P_r$  is the product of the effective area  $\lambda^2/8\pi$ , and the power density  $S_c$  as discussed in Section II-D. Using (42), we obtain the following expression for the received power:

$$P_r = \frac{\lambda^3 Q}{16\pi^2 V} P_t \quad (43)$$

If we solve (43) for  $Q$ , then we see that the cavity  $Q$  can be determined from a measurement of the power ratio  $P_r/P_t$

$$Q = \frac{16\pi^2 V P_r}{\lambda^3 P_t} \quad (44)$$

Equation (44) is commonly used for measuring the  $Q$  of reverberation chambers [18].

## V. COMPARISONS WITH MEASUREMENTS

We constructed a rectangular cavity (which we call the FAA cavity) of the geometry shown in Fig. 4 for measurements to validate the theoretical model. The cavity dimensions are  $l = 1.75$  m,  $w = 0.629$  m, and  $h = 0.514$  m, and the wall material is an aluminum alloy. The wall conductivity measured at NIST [6] was  $8.83 \times 10^6$  S/m, and we used that value in all of the calculations to follow. We used a rotating stirrer to generate statistical data, and we used average values for comparison with the theory.

To introduce absorption loss in the cavity, we used spherical glass containers of salt water. The salt concentration was selected to be that of sea water so that we could use the electrical properties of salt water given by Saxton and Lane [19]. The electrical properties are similar to those of the human body, and the frequency dependent properties are discussed in Appendix II.

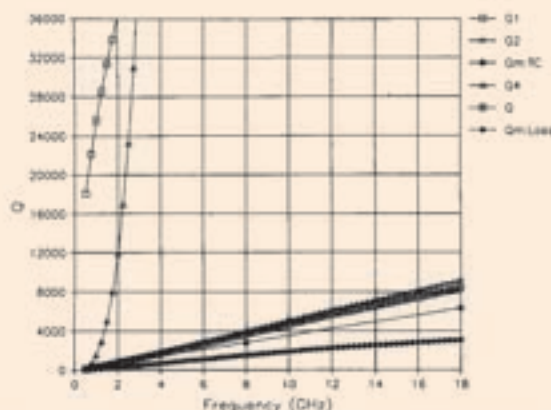


Fig. 5. Calculated and measured  $Q$  for the FAA cavity with a circular aperture of radius 1.4 cm and three salt-water spheres of radius 6.6 cm.  $Q_1$ ,  $Q_2$ , and  $Q_4$  are calculated from wall loss, absorption, and antenna reception.  $Q_3$  from aperture leakage is off scale.

In Figs. 5–7, we show comparisons of calculated and measured values of  $Q$ , the time constant, and SE for the FAA cavity with a circular aperture of radius 1.5 cm and three salt-water spheres of radius 6.6 cm. We used broadband, double-ridged horns for the transmission and receiving horns for measurements from 1 to 18 GHz. The calculations run from 0.5 to 18 GHz. Fig. 5 shows the calculated  $Q$  and the  $Q_i$  components due to the various loss mechanisms described in Section II. To make up for the extra surface area of the stirrer, the antennas, and cables, we have added 10% to the wall surface area in the calculations. Also, we have subtracted 20% from the volume ( $lwh$ ) of the empty cavity to account for volume that is taken up by the antennas, lossy spheres, stirrer, and cables. (This adjustment was also made in the calculated values in Figs. 6–10.) The measured  $Q_m$ : Loss was determined from the power ratio as given by (44). The measured  $Q_m$ : TC was determined from the time constant relationship  $Q = \omega\tau$ , as discussed in Section IV-B. The time-constant method of measuring  $Q$  is less sensitive to loss in the transmitting and receiving antennas and agrees more closely with the calculated value. The loss-ratio method of measuring  $Q$  is sensitive to unknown losses in the transmitting and receiving antennas and generally gives  $Q$  values well below the calculated values [4], [13].

Fig. 6 shows a comparison of measured and calculated time constants. The time constant measurement was made by measuring the decay time of the received pulse when the cavity was excited with a 1- $\mu$ s pulse of RF. The received waveform was averaged over stirrer position, and the details of the measurement method are given in [6].

Fig. 7 shows a comparison of calculated SE with SE measured in a reverberation chamber. The FAA cavity was placed in the NIST reverberation chamber [4], and the incident power density in the reverberation chamber was monitored with another broadband horn. In this measurement, only one of the antennas inside the FAA cavity was needed for reception, and the other antenna was left inside the cavity, but not used. To check for field uniformity, we confirmed that either antenna

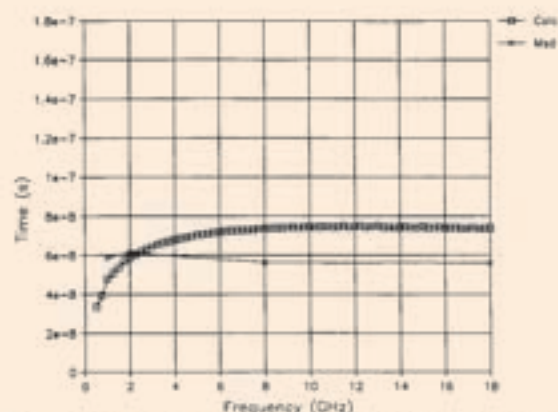


Fig. 6. Calculated and measured time constants for the FAA cavity with a circular aperture of radius 1.4 cm and three salt-water spheres of radius 6.6 cm.

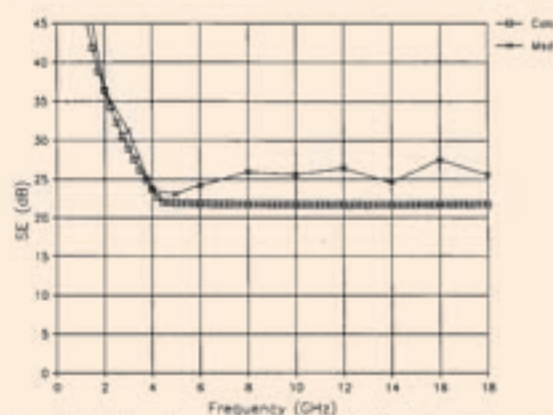


Fig. 7. Calculated and measured SE for the FAA cavity with a circular aperture of radius 1.4 cm and three salt-water spheres.

could be used as the receiving antenna with no change in the SE results. The agreement with theory is qualitatively good, but the measured SE values are higher above 5 GHz. This is consistent with the result that the measured  $Q$  is lower than the calculated value in Fig. 4.

To achieve better agreement between measurements and theory, we did another set of measurements from 12 to 18 GHz with standard-gain horn antennas. These antennas are more efficient than the broadband horns, and their smaller size allowed us to position them farther from the cavity walls. We also shortened the cables and removed the glass containers and other support material from the cavity. Comparisons between theory and measurements are shown in Figs. 8–10. In these cases we applied the same 10% surface area increase, but only a 5% volume decrease to the calculations.

The  $Q$  values in Fig. 8 are much higher without the lossy spheres, and the agreement between theory and measurements is better. The time-constant method still gives better agreement, but both methods give acceptable agreement. The time-constant agreement in Fig. 9 and the SE agreement in Fig. 10 are also improved. The improved agreement with the smaller, lower loss, standard-gain horns indicates that they

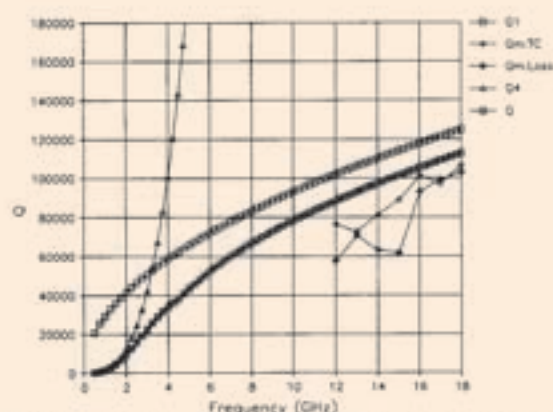


Fig. 8. Calculated and measured  $Q$  for the FAA cavity with a circular aperture of radius 1.4 cm.  $Q1$  and  $Q4$  are calculated from wall loss and antenna reception.  $Q3$  from aperture leakage is off scale. Standard-gain horns were used for measurements from 12 to 18 GHz.

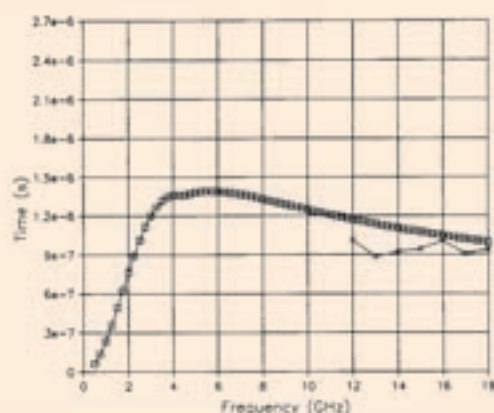


Fig. 9. Calculated and measured time constant for the FAA cavity with an aperture of radius 1.4 cm.

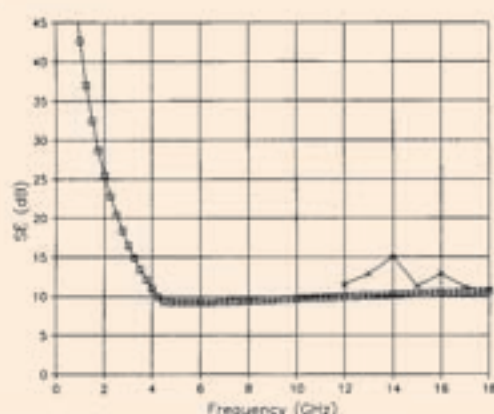


Fig. 10. Calculated and measured SE for the FAA cavity with a circular aperture of radius 1.4 cm.

might be useful in providing improved agreement with theory in reverberation chamber applications [4].

We also did a comparison of theory with SE measurements made at the Naval Surface Warfare Center (NSWC). The

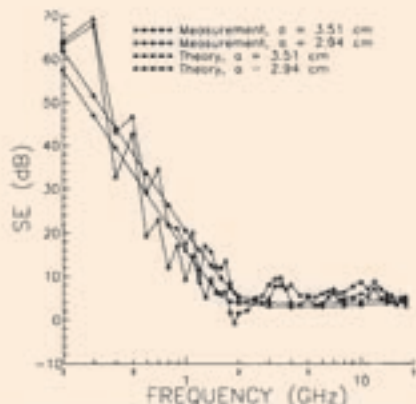


Fig. 11. Calculated and measured SE for the NSWC rectangular cavity with a circular aperture of radius  $a$ .

NSWC cavity is made of the same aluminum alloy and has the following dimensions:  $l = 1.213$  m,  $w = 0.603$  m, and  $h = 0.937$  m. The comparisons between theory and measurements for two different aperture radii,  $a = 2.94$  and  $3.51$  cm, are shown in Fig. 11. The cavity contained a stirrer and a single receiving antenna (broadband horn or a long wire for frequencies below 1 GHz). The theory is not valid below 400 MHz where the cavity is not electrically large, but the agreement is generally good over the entire frequency range.

## VI. CONCLUSION

We have presented a theory based on power balance for aperture excitation of electrically large, lossy cavities. The theory yields expressions for shielding effectiveness, cavity  $Q$ , and cavity time constant, but does not give the fine structure of the fields (standing waves, etc.) within the cavity. The advantage of the theory is that it does not require the detailed geometry of the cavity, absorbers, and apertures, but only requires a few defining parameters (cavity volume and surface area, wall conductivity, aperture transmission cross section, and absorption cross section of objects within the cavity).

The theory actually yields ensemble averages for quantities of interest (SE,  $Q$ , and  $\tau$ ), and the ensemble can be considered to represent different cavity geometries. Experimentally, the ensemble average is obtained by use of a mode stirrer within the cavity, and that is how the experimental data for SE,  $Q$ , and  $\tau$  were obtained in Section V. The agreement of the theory with the broadband experimental data was good, but a great deal of effort was required to account for additional losses that lowered measured  $Q$  and  $\tau$  and increased measured SE. The theory and measurements of  $Q$  and  $\tau$  have application to improved characterization of reverberation chambers [4], [20] where the losses have been difficult to calculate.

A number of other extensions would be useful. Measurements for cavities with multiple apertures would provide additional checks for the theory and would more nearly model typical aircraft geometries. For modeling aircraft windows, the effects of window glass (and possibly coatings) should be included in future calculations. A fifth loss mechanism, water vapor absorption, could be added to the  $Q$  theory. This loss

has been observed in reverberation chamber measurements above 18 GHz [20]. Measurements with plane-wave excitation in an anechoic chamber would provide additional checks for the angular and polarization features of the aperture theory. Also, measurements on an actual aircraft would be useful in determining whether additional features need to be added to the model.

Further experimental and theoretical studies of the statistical properties of fields in large cavities need to be performed. Such studies would be useful in extending the present theory to include probability density and distribution functions [21] in addition to average values. Some theoretical work on the statistical properties of fields in cavities [22], [23] has been done, but a more complete statistical electromagnetic theory is needed.

## APPENDIX I TRANSMISSION CROSS SECTION OF A SMALL CIRCULAR APERTURE

Consider a small circular aperture ( $ka \ll 1$ ) in a planar sheet as shown in Fig. 3. The transmitted fields can be written as the fields of a tangential magnetic dipole moment  $p_m$  and a normal electric dipole moment  $p_e$  that can be written as the product of an aperture polarizability times the appropriate incident field [9], [14]

$$p_m = \alpha_m H_{\text{tan}}^{\text{inc}} \quad \text{and} \quad p_e = \epsilon_0 \alpha_e E_n^{\text{inc}} \quad (\text{A1})$$

where  $H_{\text{tan}}^{\text{inc}}$  is the tangential magnetic field at the center of the short-circuited aperture and  $E_n^{\text{inc}}$  is the normal electric field at the center of the short-circuited aperture. The magnetic and electric polarizabilities,  $\alpha_m$  and  $\alpha_e$ , are given by [9], [14]

$$\alpha_m = 4a^3/3 \quad \text{and} \quad \alpha_e = 2a^3/3. \quad (\text{A2})$$

The dipole moments radiate in the presence of the ground plane (so their images are included), and the total transmitted power (radiated into one half-space) is [24]

$$P_t = \frac{4\pi\eta_0}{3\lambda^2} (k^2 |p_m|^2 + |p_e|^2). \quad (\text{A3})$$

We consider the cases of parallel and perpendicular polarizations separately. For parallel polarization, the short-circuited fields are

$$H_{\text{tan}}^{\text{sc}} = 2H_i \quad \text{and} \quad E_n^{\text{sc}} = 2E_i \sin \theta^i \quad (\text{A4})$$

where the incident fields can be related to the incident power density  $S_i$  by

$$S_i = \eta_0 H_i^2 \quad \text{and} \quad S_i = E_i^2 / \eta_0. \quad (\text{A5})$$

From (A1)–(A5), we can write the transmission cross section for parallel polarization as

$$\sigma_{t \text{ par}} = P_t / S_i = \frac{64}{27\pi} k^4 a^6 (1 + \frac{1}{4} \sin^2 \theta^i) \quad (\text{A6})$$

which is the result needed in Section III-B.

For perpendicular polarization, the short-circuited fields are

$$H_{\text{tan}}^{\text{sc}} = 2H_i \cos \theta^i \quad \text{and} \quad E_n^{\text{sc}} = 0. \quad (\text{A7})$$

From (A1)–(A3), (A5), and (A7), we can write the transmission cross section for perpendicular polarization as

$$\sigma_{\perp \text{ perp}} = \frac{64}{27\pi} k^4 a^6 \cos^2 \theta^i \quad (\text{A8})$$

which is the other result needed in Section III-B.

#### APPENDIX II ELECTRICAL PROPERTIES OF SALT WATER

The electrical properties of salt water have been investigated by Saxton and Lane [19] as a function of frequency, salt concentration, and temperature. The relative complex dielectric constant  $\epsilon_{cr}$  can be approximated by a combination of Debye relaxation and dc conductivity

$$\epsilon_{cr} = \frac{\epsilon_s - \epsilon_\infty}{1 + \omega^2 \tau_r^2} + \epsilon_\infty - j \left[ \frac{\sigma}{\omega \epsilon_0} + \frac{(\epsilon_s - \epsilon_\infty) \omega \tau_r}{1 + \omega^2 \tau_r^2} \right] \quad (\text{A9})$$

where  $\omega$  is the angular frequency and  $\epsilon_0$  is the permittivity of free space. The remaining parameters that characterize salt water are: static dielectric constant  $\epsilon_s$ , high-frequency dielectric constant  $\epsilon_\infty$ , dielectric relaxation time  $\tau_r$ , and dc conductivity  $\sigma$ .

The real part of the relative dielectric constant varies from  $\epsilon_s$  at low frequencies to  $\epsilon_\infty$  at high frequencies. The imaginary part consists of two terms that represent conduction loss and dielectric relaxation loss. The dielectric relaxation loss reaches its maximum at  $\omega = 1/\tau_r$ . To represent sea water at room temperature (20°C), we select the following values for the parameters [18]:  $\epsilon_s = 70.0$ ,  $\epsilon_\infty = 4.9$ ,  $\tau_r = 9.2 \times 10^{-12}$  s, and  $\sigma = 4.0$  S/m. The results from (A9) using these parameters are consistent with more recent investigations of electrolytic solutions [25].

#### ACKNOWLEDGMENT

The authors would like to thank M. Hatfield, NSWC, for providing shielding effectiveness data for the NSWC cavity and R. Geyer, NIST, for performing the wall conductivity measurement for the FAA cavity.

#### REFERENCES

- [1] "Guidance to certification of aircraft electrical/electronic systems for operation in the high intensity radiated fields (HIRF) environment," Society of Automotive Engineers, SAE AE4R Committee Rep., July, 1991.
- [2] A. Taflov and K. Umashankar, "A hybrid moment method/finite-difference time-domain approach to electromagnetic coupling and aperture penetration into complex geometries," *IEEE Trans. Antennas Propagat.*, vol. AP-30, pp. 617–627, 1982.
- [3] R. E. Richardson, "Mode-stirred chamber calibration factor, relaxation time, and scaling laws," *IEEE Trans. Instrum. Meas.*, vol. IM-34, pp. 573–580, 1985.
- [4] M. L. Crawford and G. H. Koepke, "Design, evaluation, and use of a reverberation chamber for performing electromagnetic susceptibility/vulnerability measurements," Nat. Bur. Stand. (U.S.) Tech. Note 1092, 1986.
- [5] J. M. Dunn, "Local, high-frequency analysis of the fields in a mode-stirred chamber," *IEEE Trans. Electromagn. Comput.*, vol. 32, pp. 53–58, 1990.
- [6] D. A. Hill, J. W. Adams, M. T. Ma, A. R. Ondrejka, B. F. Riddle, M. L. Crawford, and R. T. Johnk, "Aperture excitation of electrically large, lossy cavities," Nat. Inst. Stand. Tech. (U.S.) Tech. Note 1361, 1993.

- [7] B. H. Liu, D. C. Chang, and M. T. Ma, "Eigenmodes and the composite quality factor of a reverberating chamber," Nat. Bur. Stand. (U.S.) Tech. Note 1066, 1983.
- [8] H. C. Van de Hulst, *Light Scattering by Small Particles*. New York: Dover, 1981.
- [9] D. A. Hill, M. L. Crawford, M. Kanda, and D. I. Wu, "Aperture coupling to a coaxial air line: Theory and experiment," *IEEE Trans. Electromagn. Comput.*, vol. 35, pp. 69–74, 1993.
- [10] C. M. Butler, Y. Rahmat-Samii, and R. Mitra, "Electromagnetic penetration through apertures in conducting surfaces," *IEEE Trans. Antennas Propagat.*, vol. AP-26, pp. 82–93, 1978.
- [11] C. T. Tai, "On the definition of effective aperture of antennas," *IEEE Trans. Antennas Propagat.*, vol. AP-9, pp. 224–225, 1961.
- [12] D. A. Hill and M. H. Francis, "Out-of-band response of antenna arrays," *IEEE Trans. Electromagn. Comput.*, vol. EMC-29, pp. 282–288, 1987.
- [13] T. A. Loughry, "Frequency stirring: an alternate approach to mechanical mode-stirring for the conduct of electromagnetic susceptibility testing," Phillips Laboratory, Kirtland Air Force Base, NM, Tech. Rep. PL-TR-91-1036, 1991.
- [14] H. A. Bethe, "Theory of diffraction by small holes," *Phys. Rev.*, vol. 66, pp. 163–182, 1944.
- [15] J. Meixner and M. Andrejewski, "Strenge theorie der beugung ebener elektromagnetischer wellen an der vollkommen leitenden kreisscheibe und an der kreisförmigen öffnung im vollkommen leitenden eben schirm," *Ann. Physik*, vol. 7, pp. 157–168, 1950.
- [16] H. Levine and J. Schwinger, "On the theory of electromagnetic wave diffraction by an aperture in an infinite plane conducting screen," *Commun. Pur Appl. Math.*, vol. 3, pp. 355–391, 1950.
- [17] K. S. H. Lee and F.-C. Yang, "Trends and bounds in RF coupling to a wire inside a slotted cavity," *IEEE Trans. Electromagn. Comput.*, vol. 34, pp. 154–160, 1992.
- [18] P. Coena, G. Latmiral, and E. Paolini, "Performance and analysis of a reverberating enclosure with variable geometry," *IEEE Trans. Electromagn. Comput.*, vol. EMC-22, pp. 2–5, 1980.
- [19] J. A. Saxton and J. A. Lane, "Electrical properties of sea water," *Wireless Engineer*, vol. 29, pp. 269–275, 1952.
- [20] M. L. Crawford, M. T. Ma, J. M. Ladbury, and B. F. Riddle, "Measurement and evaluation of a TEM/reverberating chamber," Nat. Inst. Stand. Tech. (U.S.) Tech. Note 134, 1990.
- [21] J. G. Kostas and B. Boveris, "Statistical model for a mode-stirred chamber," *IEEE Trans. Electromagn. Comput.*, vol. 33, pp. 366–370, 1991.
- [22] R. H. Price, H. T. Davis, R. H. Bonn, E. P. Wenaas, R. Achenbach, V. Gieri, R. Thomas, J. Alcalá, J. Hanson, W. Haynes, C. McCrea, C. Montano, R. Peterson, B. Trautlein, and R. Umber, "Determination of the statistical distribution of electromagnetic field amplitudes in complex cavities," JAYCOR Rep. 88JAL129, 1988.
- [23] T. H. Lehman, "A statistical theory of electromagnetic fields in complex cavities," EMP Interaction Note 494, May 1993.
- [24] R. F. Harrington, *Time-Harmonic Electromagnetic Fields*. New York: McGraw-Hill, 1961.
- [25] J. B. Hasted, *Aqueous Dielectrics*. London: Chapman and Hall, 1973, ch. 6, "Electrolytic Solutions."



David A. Hill (M'72-SM'76-F'87) was born in Cleveland, OH, on April 21, 1942. He received the B.S.E.E. and M.S.E.E. degrees from Ohio University, Athens, in 1964 and 1966, respectively, and the Ph.D. degree in electrical engineering, from Ohio State University, Columbus, in 1970.

Since 1970 he has been a member of the Boulder, CO, scientific community. From 1970 to 1971 he was a Visiting Fellow with the Cooperative Institute for Research in Environment Sciences, where he worked on pulse propagation. From 1971 to 1982 he was with the Institute for Telecommunication Sciences, where he worked on theoretical problems in antennas and propagation. Since 1982 he has been in the Electromagnetic Fields Division of the National Bureau of Standards and Technology where he has been working on EMC/EMI and remote sensing problems. He is also a Professor Adjoint in the Department of Electrical and Computer Engineering at the University of Colorado.

Dr. Hill is a member of URSI Committees A, B, E, and F. He has served as an Associate Editor for the IEEE TRANSACTIONS ON GEOSCIENTIFIC AND REMOTE SENSING and the IEEE TRANSACTIONS ON ANTENNAS AND PROPAGATION.



**Mark T. Ma** (S'58-M'62-SM'65-F'82) received the Ph.D. degree in electronic engineering from Syracuse University, Syracuse, NY, in 1961.

He is currently a Senior Electrical Engineer with the National Bureau of Standards and Technology, Boulder, CO, and a Professor Adjoint at the University of Colorado. He published about 100 journal papers and reports on antennas, wave propagation, telecommunications, and electromagnetic interference. He also authored a book *Theory and Application of Antenna Arrays* (New York: Wiley, 1974) and contributed chapters in *Antenna Engineering Handbook* and *Research Topics in Electromagnetic Wave Theory*.

1974) and contributed chapters in *Antenna Engineering Handbook* and *Research Topics in Electromagnetic Wave Theory*.

**Bill F. Riddle**, photograph and biography not available at the time of publication.

**Myron L. Crawford** (M'79-SM'81-F'90), photograph and biography not available at the time of publication.

**Arthur R. Ondrejka**, photograph and biography not available at the time of publication.

**Robert T. Johnk** (M'91), photograph and biography not available at the time of publication.

EMC

## REVERBERATION CHAMBER THEORY/EXPERIMENT SHORT COURSE

March 30-April 3, 2009

OKLAHOMA STATE UNIVERSITY

Location: OSU-Stillwater, OK

Time: 8.00AM to 5.00PM

Fee: \$2500 if registered before February 27, 2009

\$2750 if registered after February 27, 2009

4.0 CEUs/40 PDHs

<http://rc-course.okstate.edu>

### Host

The course is hosted by the School of Electrical and Computer Engineering of Oklahoma State University. Technical and equipment support is provided by the Naval Surface Warfare Center, Dahlgren Division (NSWCDD), Dahlgren, VA.

### About the Course

Several standards including MIL-STD-461E, RTCA DO 160D, IEC 61000-21, and SAE J551/J113 permit the use of reverberation chambers for EMC certification testing. This course is designed for engineers and technicians who will be involved in radiated emission or immunity testing of commercial or military systems using reverberation chambers. The course will also be valuable to personnel evaluating the use of reverberation chambers as a complement to or replacement for other types of radiated test facilities.

The theory portion covers the statistical nature of reverberation chamber testing, characterization of the EM test conditions, and the tradeoff between uncertainty in test results and test time. The experimental portion includes demonstrations, test setups and instrumentation, statistical sampling techniques (mechanical tuner operation and frequency sweeps), and chamber characterization and calibration measurements. While the experimental portion includes reverberation chamber demonstrations it consists primarily of a series of hands-on experiments conducted in small groups of four to five people. The notes format includes the objective, a description of the experiment, instrumentation, test setup, procedures, and room for specific measurements, analyses, results, and conclusions. The experiments and demonstrations are conducted in the small (2.5 x 4 x 7 feet) OSU reverberation chamber and an ETS-Lindgren SMART 80 chamber. The small chamber, constructed in-house by OSU students for less than \$1000, indicates the flexibility of the reverberation chamber concept. The small chamber can be used for radiated immunity and emission testing above 1 GHz in accordance with several standards. The chamber demonstrates the statistical equivalence of the electromagnetic environment in all conductive cavities independent of size and construction materials. Participants will have a thorough understanding of the operation of a reverberation chamber for EMC testing. They will have developed a test plan for an immunity test with specified conditions and objectives. They will also have a permanent record of data collected and analyzed, and an extensive set of notes.

### Contact

Dr. Charles F. Bunting. Email: [reverb@okstate.edu](mailto:reverb@okstate.edu)

Dr. Gus Freyer. Email: [gfreyer@earthlink.net](mailto:gfreyer@earthlink.net)